JMEPEG (1995) 4:175-181

Effects of Molten Aluminum on H13 Dies and Coatings

M. Yu, R. Shivpuri and R.A. Rapp

The effects of molten aluminum casting alloy A390 on a commercially heat treated H13 die steel and two wear-resistant coatings, $Cr_{23}C_6$ and TiN, were investigated by an accelerated corrosion test. The H13 steel suffered severe corrosion due to the rapid formation of intermetallic compounds. The formation of multilayer intermetallic compounds and the simultaneous dissociation of the intermetallic compound τ_6 (Al_4FeSi) were attributed to the fast dissolution of H13 steels into the melt. This dissolution of the H13 steel was accelerated dramatically by turbulence and an increase in melt temperature. Significant improvement in corrosion resistance was achieved for the H13 steel coated by $Cr_{23}C_6$ via a pack cementation process.

Keywords

accelerated corrosion test, aluminum casting alloy A390, corrosion, $Cr_{23}C_6$, die casting, dissolution, H13 die steel, intermetallic compound, melt temperature, melt turbulence, molten aluminum, TiN, wear resistant coating

1. Introduction

ACCELERATED dissolution "washout" and soldering of die casting dies are major problems in the aluminum and zinc die casting industry. Die corrosion occurs at local spots of the die surface at high temperature. This corrosion involves both reaction and mutielement diffusion and is difficult to prevent because of the high temperature of a die casting operation. Surface coating of the die steel is an approach to reduce the die failure and extend the service life of dies. An understanding of die corrosion by the aggressive molten aluminum attack is important and necessary to select a coating for the H13 die or an effective die spray lubricant. Figure 1 illustrates the microstructure of A390 (aluminum casting alloy) soldering on an H13 (a common die steel) test pin after 1000 shots of a die casting campaign.

Microhardness test and energy dispersive spectroscopy (EDS) results revealed that the compound layer formed between the soldered A390 and H13 substrate is the intermetallic compound $\tau_6(Al_4FeSi)$ with a microhardness of 639 HV (Ref 1). According to the Al-Fe-Si ternary diagram (Ref 2), this compound is formed in the range of 577 to 620 °C (1070 to 1148 °F), which is very close to the temperature of the die casting operation.

The chemical and mechanical bonding strength between the intermetallic layer formed at the interface and the solidified layer determines the amount of soldering. Soldering occurs when the intermetallic layers have strong bonding strength. However, accelerated dissolution results from continuous metal loss due to dissociation and detachment of the intermetallic layer formed during the casting operation. Both soldering and accelerated dissolution deteriorate the die surface and the resulting quality of the casting.

The objective of this investigation was to study the corrosive effects of molten aluminum alloy on the H13 die material, to understand better the inherent die failure mechanisms that lead to premature failure due to "washout" or soldering, and finally to evaluate the performance of two wear resistant coatings, $Cr_{23}C_6$ by a diffusion grown pack cementation and TiN by a sputtering process. A rotating immersion test was used to carry out this investigation.

2. Experimental Materials and Procedure

2.1 *Materials*

Standard non-heat-treated H13 pins (28 HRC) of 9.525 mm (0.375 in.) diameter by 76.2 mm (3 in.) length were used in all pack cementation coating experiments. The hot worked H13 tool steel contains 0.40 wt% C, 1.05 wt% Si, 5.00 wt% Cr, 1.35 wt% Mo, and 1.10 wt% V with the remainder iron. The pins were commercially heat treated as follows: stress relieved for 0.5 h at 537 °C (1000 °F) and vacuum hardened for 90 h at 1024 °C (1875 °F) with as quenched hardness of 52 HRC. They were then tempered for 3 h at 537 °C (1000 °F) and retempered for 3

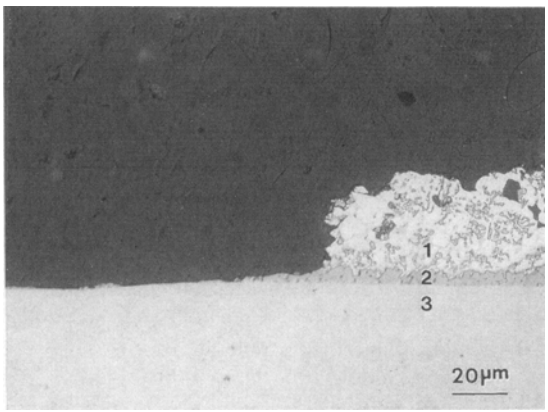

Fig. 1 Cross-sectional microstructure of H13 pin with A390 soldering after 1000 shots on H-250B cold chamber die casting machine at Ohio State University. 400×. (1) A390. (2) τ_6. (3) H13

M. Yu and **R. Rapp,** Department of Materials Science and Engineering, The Ohio State University, Columbus, OH 43210, USA; and **R. Shivpuri,** Department of Industrial and Systems Engineering, The Ohio State University, Columbus, OH 43210, USA.

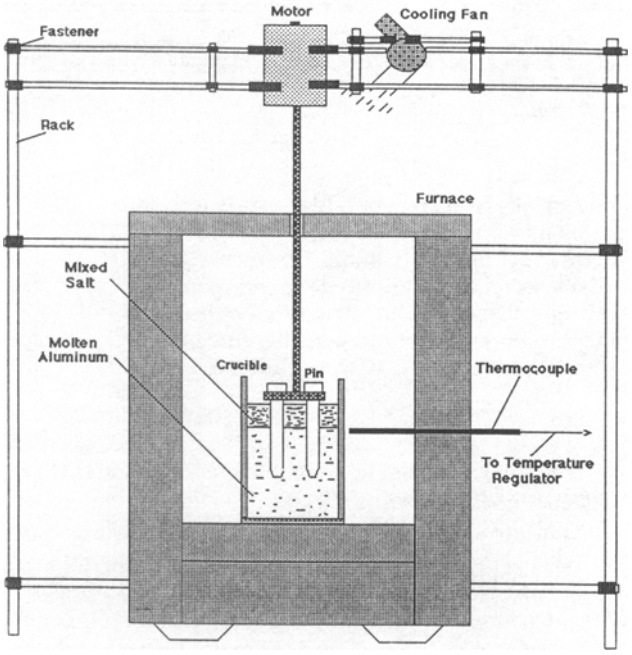

Fig. 2 Schematic diagram of accelerated corrosion test.

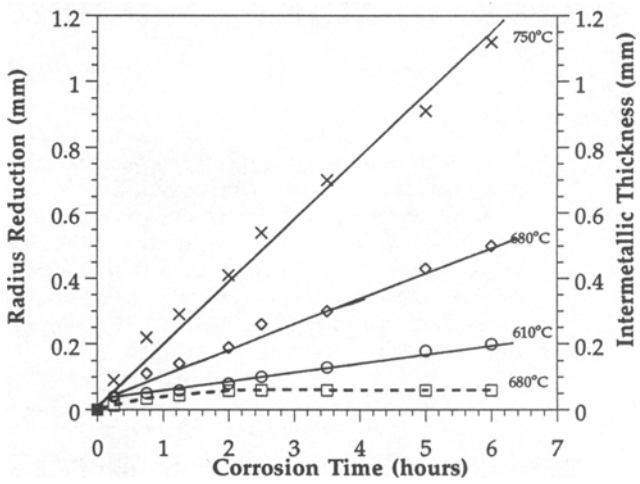

Fig. 3 Effects of melt temperature and corrosion time on the dissolution of H13 pins. Solid line is radius reduction. Dashed line is intermetallic layer thickness at 680 °C.

h at 537 °C (1100 °F) and 3 h at 537 °C (1000 °F) to a final hardness of 46 to 48 HRC.

The $Cr_{23}C_6$ coating on the test pin was achieved by a $AlCl_3$-activated diffusion pack cementation process at 1050 °C for 16 h (Ref 3). A 15 μm uniform $Cr_{23}C_6$ coating (1550 HV) was formed on the H13 substrate (45.5 HRC). The TiN coating (2.5 μm) on the H13 test pin was applied using a low-temperature physical vapor deposition process (Ref 4).

Aluminum alloy A390 was used for accelerated erosion and corrosion experiments. The hypereutectic A390 alloy has the composition of 16.0 to 18.0 wt% Si, 4.0 to 5.0 wt% Cu, 0.6 to 1.1 wt% Fe, 0.50 to 0.65 wt% Mg, 0.10 wt% Zn, 0.20 wt% Ti, and remainder aluminum. On cooling the A390 melt, the primary Si precipitates first above the eutectic temperature at 577 °C and is followed by the solidification of the Al-Si eutectic. The primary silicon precipitates as an irregular blocky shape. The eutectic silicon, known as secondary silicon, is finely distributed in the α_{Al} phase. Because of rapid heat transfer between the casting alloy and the die surface during the solidification, a supercooling at the surface of the casting A390 develops. Therefore, the primary Si preferentially precipitates at the interface between the H13 die and the casting alloy A390.

2.2 *Test Setup and Procedure*

An accelerated corrosion test was set up to evaluate the dissolution rate of H13 pins in both static and agitated melts. Figure 2 is a schematic diagram of accelerated corrosion test setup. Four test pins were held symmetrically in the rotating disc (radius 2.5 cm) driven by an electric motor. A390 blocks (1.5 kg) with 285 g of mixed salts (135 g NaCl + 135 g KCl + 15 g NaF) were premelted in a crucible placed in the center of the furnace. The salt solution was used to minimize the oxidation of the melt. The speed of rotation was varied to study the effects of fluid flow on the attack by molten aluminum. Test pins were air quenched after a desired corrosion time. A 2 wt% NaOH solution was used to clean the test pins after quenching. The soldered aluminum and the intermetallic compounds (Al-Fe-Si) formed during the corrosion test were completely cleaned by the NaOH solution by dipping for 12 h to two days. The recession (reduction) of the test pin radius was measured after cleaning. The test pins were also cut, mounted, polished, and etched for metallurgical examination.

This corrosion test was accelerated by: (a) conducting tests at much higher temperatures (680 to 750 °C, 1256 to 1383 °F) than those in commercial die casting operations (500 to 600 °C, 932 to 1112 °F) during the die holding period; and (b) dipping and rotating the pins in the molten aluminum bath for up to 6 h while the actual contact time between H13 and molten aluminum alloys is less than 1 s per cycle in an actual die casting campaign. The accelerated corrosion test provided a platform for an efficient evaluation of the dissolution and soldering resistance of the test pins in molten A390 casting alloy for different test conditions in a reasonable test period.

3. Results of Corrosion Tests

3.1 *H13 Steel in Static A390 Melt*

Accelerated corrosion tests were conducted to investigate the isothermal dissolution rate of H13 pins in the static A390 melt at temperatures of 610, 680, and 750 °C, respectively. Corrosion times of 0.25, 0.5, 1.25, 2.0, 2.5, 3.0, 3.5, 5.0, and 6 h were used for each test temperature. The intermetallic layers and soldered A390 were removed with NaOH cleaning. Effects of melt temperature and corrosion time on the dissolution of

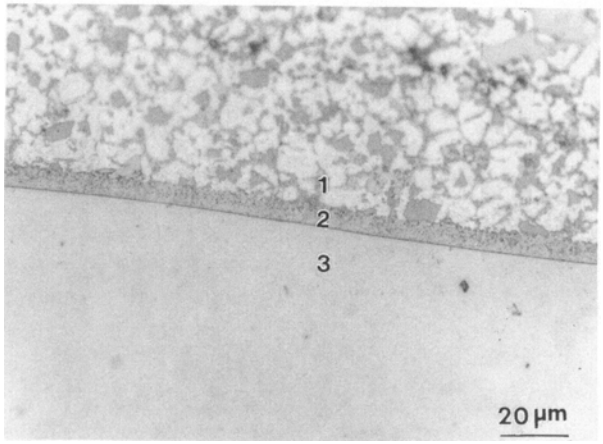

(a)

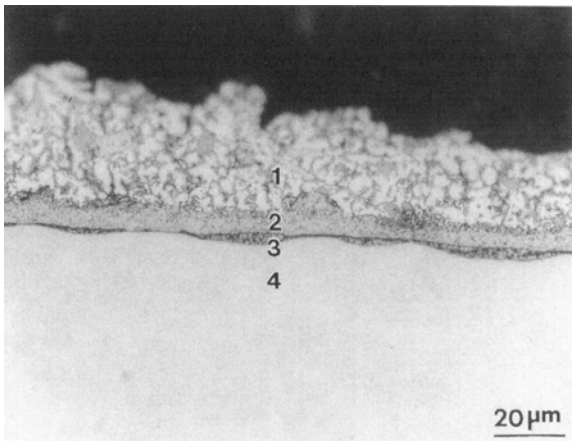

(b)

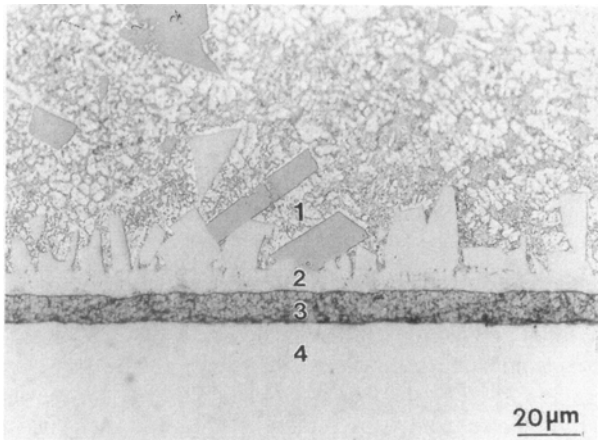

(c)

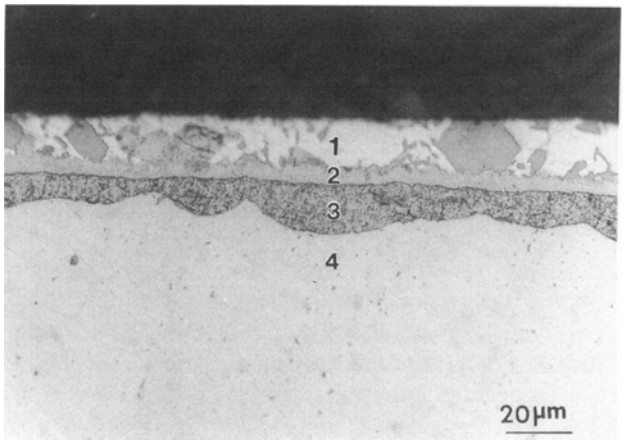

(d)

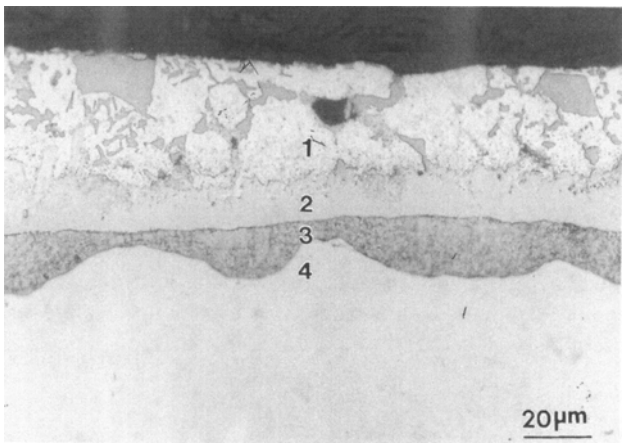

(e)

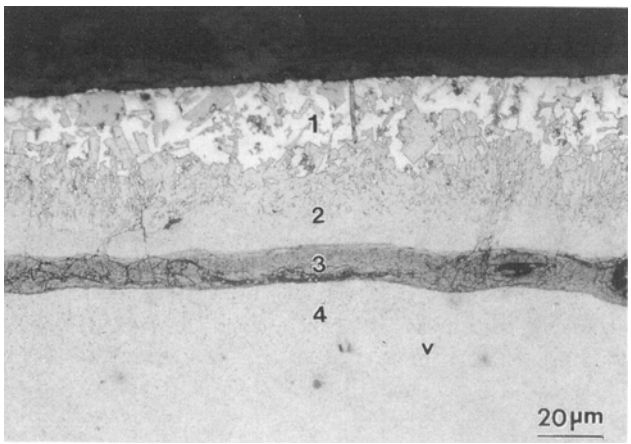

(f)

Fig. 4 Cross-sectional micrographs after (a) 0.25 h (b) 0.75 h (c) 1.25 h (d) 2.0 h (e) 2.5 h (f) 3.5 h (g) 5.0 h, and (h) 6.0 h of corrosion test in the static A390 melt at 680 °C (400×). For (a), 1 is A390; 2 is τ_6; 3 is H13. For (b)-(f), 1 is A390; 2 is τ_6; 3 is τ_5; 4 is H13. For (g)-(h), 1 is A390; 2 is τ_6; 3 is τ_5; 4 is τ_2; 5 is H13.(continued)

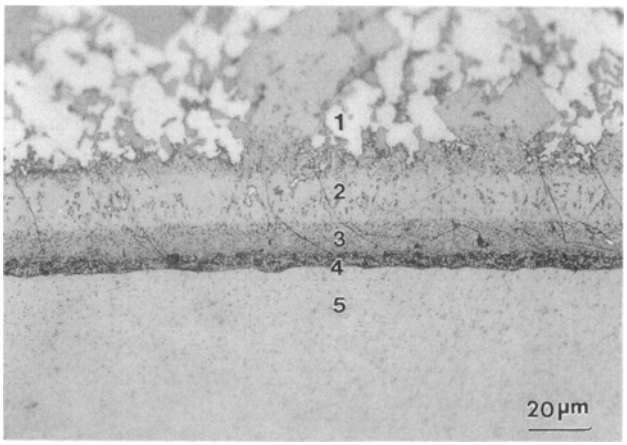

(g)

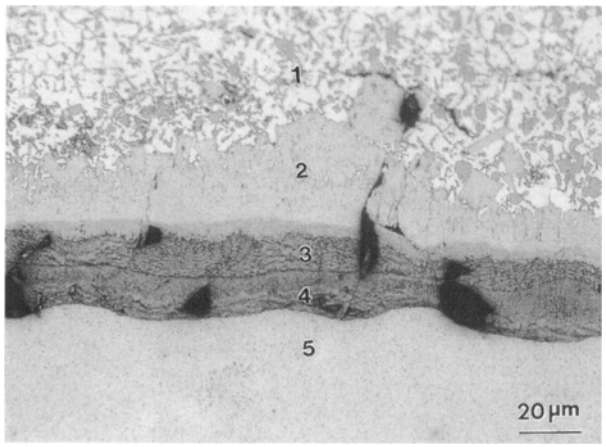

(h)

Fig. 4 (continued) Cross-sectional micrographs after (a) 0.25 h (b) 0.75 h (c) 1.25 h (d) 2.0 h (e) 2.5 h (f) 3.5 h (g) 5.0 h, and (h) 6.0 h of corrosion test in the static A390 melt at 680 °C (400×). For (a), 1 is A390; 2 is τ_6; 3 is H13. For (b)-(f), 1 is A390; 2 is τ_6; 3 is τ_5; 4 is H13. For (g)-(h), 1 is A390; 2 is τ_6; 3 is τ_5; 4 is τ_2; 5 is H13.

H13 pins are shown in Fig. 3, which also includes the thickness of the intermetallic layer at 680 °C.

The H13 pins for the accelerated corrosion tests at 680 °C at various corrosion times were not NaOH cleaned, but cut, mounted, and polished for metallurgical analyses. Figures 4(a-h) are the cross-sectional microstructures of H13 pins.

One distinct intermetallic layer was observed for a short contact time of H13 and the A390 melt, such as 0.25 h (Fig. 4a). This intermetallic layer was identified as τ_6 (Al_4FeSi) from EDS analysis. Two distinct intermetallic layers identified as τ_6 (Al_4FeSi) and τ_5 ($Al_{15}Fe_6Si_5$) were formed after 0.75, 1.25, 2.0, 2.5, and 3.5 h of corrosion as shown in Fig. 4(b-f). Three intermetallic layers, τ_6, τ_5, and τ_2 ($Al_{12}Fe_6Si_5$) were found after 5.0 h (Fig. 4g) and 6.0 h (Fig. 4h).

The thickness of the intermetallic layers increased sharply from start to 2.0 h, but remained approximately constant at the longer corrosion times at 680 °C as shown in Fig. 3. The continuous dissolution of outer intermetallic layer τ_6 was observed. The loss of τ_6 was compensated by the further growth of $\tau 6$ because of the reaction of τ_5 with the Al diffused from the melt. The inner layer τ_5 was formed from the reaction of the τ_2 and diffused Al from the melt. The continuous reaction between H13 and the diffused Al from melt maintained a constant thickness of τ_2 after 5 h of corrosion time. Therefore, the creation and conversation of adjacent layers by the Al and Fe diffusion kept the total intermetallic layer thickness constant as shown in Fig. 3.

3.2 *H13 in Agitated A390 Melt*

The effect of melt flow velocity was investigated by mechanically rotating the test pin and evaluating the pin diameter recession after a desired accelerated test time. Rotation speeds of 50 rpm, 100 rpm, and 175 rpm in the A390 melt at 680 °C were investigated. The results are shown in Fig. 5.

The results indicate a significant dependence of pin recession on the melt flow velocity because of rapid dissolution of intermetallic layers into the turbulent melt. Only two intermetallics, τ_6 and τ_5, could be observed for all three rotation speeds up to 6 h. A typical cross-sectional microstructure after the rotation corrosion test is illustrated in Fig. 6. A thin τ_6 layer with 11 μm thickness and a much thinner τ_5 layer with 1 μm thickness were identified for the 5 h corrosion test at the 175 rpm. The rapid agitation of melt adjacent to the intermetallic layer prevents thickening of the outer τ_6 layer. The diffusion flux of aluminum through the thin τ_6 (29.1 wt% Fe) layer prevented the formation of a thick intermetallic τ_2 because appreciable Fe diffusion is needed to form the intermetallic τ_2, which has high Fe content (41.9 wt%).

The intermetallic thicknesses in the three agitated melts are shown in Fig. 7. The detachment of the non-protective τ_6 intermetallic layer into all the melts and the simultaneous formation of τ_6, τ_5, and τ_2 intermetallics caused recession of the pin radius at the static melt. The dissociation of the τ_6 compound into small fragments was severely accelerated by the agitated melt impingement, which resulted in very rapid pin radius recession and very thin intermetallic layers.

These observations support the hypothesis that aluminum soldering begins with the formation of intermetallic compounds; the reduction in radius results from both direct dissolution of Fe into the melt and detachment of nonprotective outer intermetallic layer τ_6.

3.3 *$Cr_{23}C_6$ and TiN Coatings*

Two test pins coated with $Cr_{23}C_6$ and TiN were evaluated in the molten A390 at 680 °C, along with the uncoated H13 pin. The test results are shown in Fig. 8. The test results indicate that $Cr_{23}C_6$-coated H13 pin achieved significant resistance to molten A390 corrosion in static melts. The TiN coating was readily dissolved in molten A390. The corrosion resistance of the TiN-coated H13 pin was not appreciably greater than the uncoated H13 test pin.

Table 1 Ternary solid phases in the Al-Fe-Si system

Ternary phase Symbol	Formula	Composition, wt% Al	Fe	Si	Homogeneity range
τ_1	$Al_3Fe_3Si_2$	26.6	55.0	18.4	...
τ_2	$Al_{12}Fe_6Si_5$	40.5	41.9	17.6	...
τ_3	$Al_9Fe_5Si_5$	36.6	42.1	21.2	2 to 3%
τ_4	Al_3FeSi_2	41.9	28.9	29.1	...
τ_5	$Al_{15}Fe_6Si_5$	46.0	38.1	16.0	5% Al
τ_6	Al_4FeSi	56.3	29.1	14.6	...

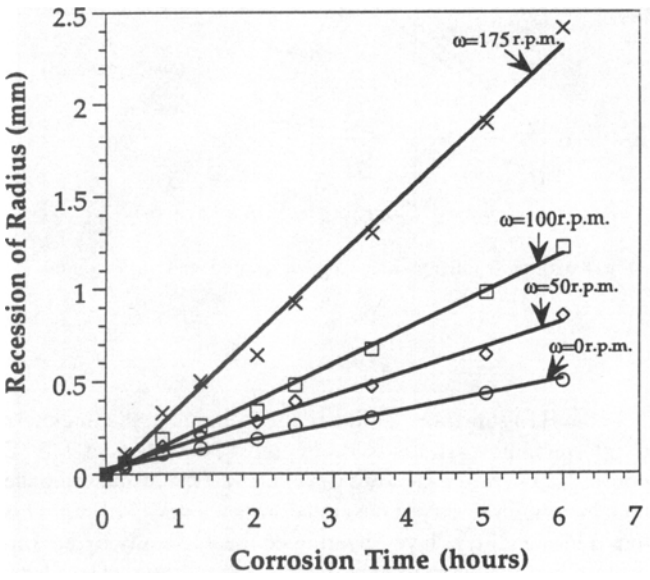

Fig. 5 Effects of rotation on the H13 pin diameter recession.

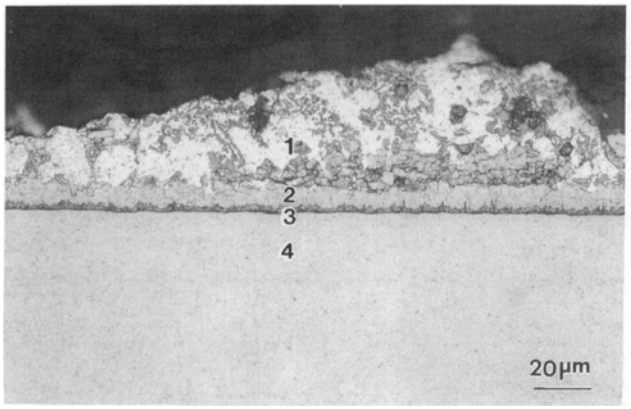

Fig. 6 Microstructure of H13 pin after 5 h of rotation at 175 rpm. (1) A390. (2) τ_6. (3) τ_5. (4) H13.

4. Discussion

4.1 *Thermodynamics of Fe-Al-Si System*

From the ternary phase diagram of Fe-Al-Si system, Table 1 lists the ternary solid phases. Intermetallic layers that can form at the die casting operating temperature range (500 to 700 °C) are: Al_4FeSi (τ_6), $Al_{15}Fe_6Si_5$ (τ_5), and Al_3FeSi_2 (τ_4). The following eutectic and peritectic reactions can occur:

$$L + \tau_4 + \tau_5 \leftrightarrow \tau_6 \text{ at } 700\ ^\circ C \quad (1)$$

$$L + \theta \leftrightarrow (Al) + \tau_5 \text{ at } 620\ ^\circ C \quad (2)$$

$$L + \tau_5 \leftrightarrow (Al) + \tau_6 \text{ at } 615\ ^\circ C \quad (3)$$

$$L + \tau_4 \leftrightarrow (Si) + \tau_6 \text{ at } 600\ ^\circ C \quad (4)$$

$$L \leftrightarrow (Al) + (Si) + \tau_6 \text{ at } 577\ ^\circ C \quad (5)$$

For 500 to 600 °C, the observation of τ_6 agreed with the eutectic and peritectic reactions (4 and 5). EDX results for the single intermetallic layer in Fig. 4(a) showed high silicon contents. The average measured composition for this intermetallic layer was 55.6 wt% Al, 15.53 wt% Si, and 28.36 wt% Fe, and 1.85 wt% Cr. These ratios of atomic percentages are very close to intermetallic compound τ_6 (Al_4FeSi).

When the contact time was increased to 0.75, 1.25, 2.0, 2.5, and 3.5 h, an additional intermetallic layer τ_5 was formed as shown in Fig. 4(b-f). EDS results for the first intermetallic layer showed negligible difference from the intermetallic compound τ_6 (Al_4FeSi). The average composition for the second intermetallic layer was 35.63 wt% Al, 15.85 wt% Si, 45.89 wt% Fe, and 2.62 wt% Cr, close to the τ_5 phase, which continued to thicken with the increase of contact time from 1 to 3.5 h. The third intermetallic compound τ_2 was formed after 5 h.

The Al/Si ratio in τ_2 is lower than that in τ_5, and Al/Si ratio in τ_5 is lower than that in τ_6. Al had to be supplied through diffusion to form τ_6 and τ_2. Obviously, both reaction and active diffusion occur between the intermetallic layers τ_6, τ_5, and τ_2. The constant intermetallic thickness of τ_6, τ_5, and τ_2 in the static melt further indicated that the dissolution of H13 continued due to the continuous dissociation and detachment of the nonprotective τ_6 layer and the sequential phase transformation of H13 to τ_2, τ_2 to τ_5, τ_5 to τ_6. These phase transformations are caused by the diffusion of Al, Si, and Fe through the intermetallic layers.

4.2 *Solubility of H13 Die Steel*

Figures 3 and 5 illustrate that the radius reduction of pins was larger than the intermetallic thickness for various H13 and A390 contact times. This indicates that the weight-loss of H13

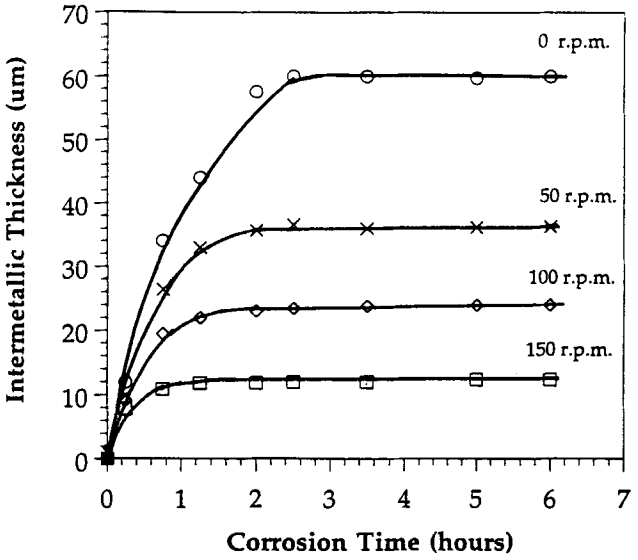

Fig. 7 Thickness of intermetallic layers in agitated A390 melt at different rotation speed.

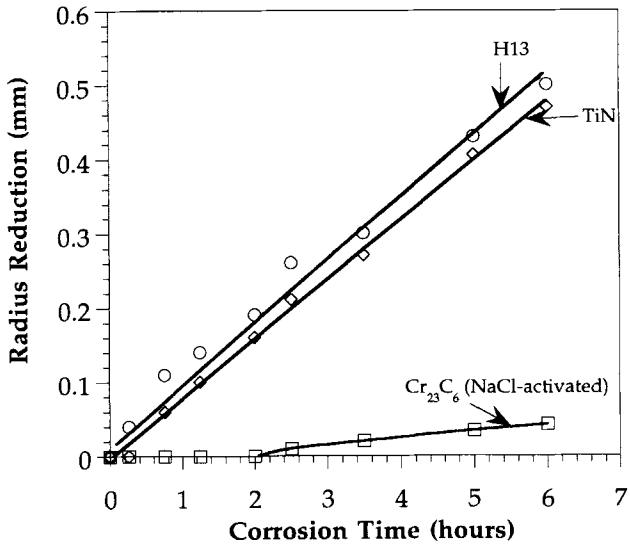

Fig. 8 Molten A390 attack on $Cr_{23}C_6$-coated and TiN-coated H13 pins.

in molten A390 is also due to factors other than the intermetallic formation, as shown in the Fig. 4. At 680 °C, about 8 wt% Fe can be dissolved into molten A390 without formation of intermetallic compounds according to the Al-Fe-Si phase diagram. H13 could dissolve into molten A390 upon the initial contact, which also contributes to the difference between the pin diameter recession and the thickness of intermetallics in Fig. 3 and 5. The H13 dissolution continued throughout the contact of H13 and A390 as indicated in Fig. 4. The intermetallic layer τ_6 was also found in the molten A390 after 1 h of H13 and A390 contact. The formation of the τ_6 layer and subsequent detachment from the H13 pin resulted in a significant weight loss and dimension reduction of H13 pins as shown in Fig. 3 and 5.

Therefore, the weight loss of H13 steel in the molten A390 alloy can be attributed to: (a) the continuous formation of solid intermetallic compounds τ_6, τ_5, and τ_2, and subsequent detachment of the outer τ_6 from the H13 substrate; and (b) direct dissolution of H13 into molten A390.

4.3 *Washout and Soldering Effects*

The terms "washout" and "erosion" are frequently used in the die casting industry to describe the dimensional loss of dies, core pins, and shot sleeves. The physical properties of these parts, such as hardness, have been long recognized as important factors to control the damage due to washout or erosion (Ref 5). The aggressive molten aluminum attack due to the formation of multiple intermetallic compounds can also significantly affect the resistance of H13 steel to dissolution. Washout can be readily observed because of rapid diffusion of Al, Si, and Fe, and the formation of intermetallic compounds, such as τ_6, τ_5, and τ_2. It can be accelerated with the increase of melt temperature and degree of melt turbulence.

Soldering occurs at local hot spots of die surface or pin head because of the strong adherence of the intermetallic compound τ_6 to the H13 substrate. Unlike in the static melt, the thickness of intermetallic τ_6 in the soldering after 1000 shots at 730 °C pouring temperature is only 5 μm (Fig. 1). This results from the high injection velocity of the melt during the cavity filling. This thin intermetallic τ_6 layer is removed mechanically by the impact of the injected melt, which results in washout. Therefore, the thick intermetallic τ_6 layer observed in dip tests is not observed in an actual die casting operation.

4.4 *Coating To Resist Washout and Soldering*

An effective wear-resistant coating on H13 should be able to eliminate or reduce the severe washout and soldering of the H13 dies, shot sleeves, or core pins. The coating on H13 pins should have the following physical and chemical properties: (a) high hardness for erosion resistance, (b) inertness to chemical and diffusion attack of molten aluminum alloys, (c) compatible match of coefficient of thermal expansion (CTE) with the H13 substrate for thermal cracking resistance, (d) nonporous, adherent metallurgical bonded diffusion coating to resist spalling, and (5) high oxidation resistance at working temperature of 500 to 650 °C. These criteria require the coating is deposited by a diffusion coating process at high temperature; that is, above the austenitic temperature of H13. The hard pack cementation $Cr_{23}C_6$ coating was grown on the H13 substrate, and excellent metallurgical bonding adherence was achieved. The compatible CTE match between $Cr_{23}C_6$ (7.6×10^{-6}/C at 650 °C) and H13 (7.3×10^{-6}/C at 650 °C) enabled this coating to withstand cracking due to thermal cycling. The $Cr_{23}C_6$ coating resisted washout or erosion. The low dissolution rate of this coating provided a barrier for H13 die steel from molten aluminum attack, and consequently, soldering of H13 steels was reduced. Finally, the superior oxidation resistance of this coating eliminated the loss of H13 die steel due to scaling.

The pack cementation diffusion coating process is an inexpensive and economically feasible process (Ref 6). However, this high-temperature coating process requires the heat treatment of substrate after coating to regain its mechanical properties. Therefore, a non-heat-treated H13 workpiece is preferred for diffusion coating, and a heat treatment after coating is required. Subsequent machining may be required for some parts with complicated geometry due to potential distortion after heat treating.

5. Conclusions

From the accelerated corrosion results of coated and uncoated H13 die steel and selected coating in molten A390 alloy, the following conclusions can be drawn:

- The weight loss and pin radius reduction area due to dissolution of Fe in the molten A390 alloy can be attributed to: (a) direct dissolution of H13 in molten A390, and (b) the formation of intermetallic layers, and their detachment from the H13 substrate.
- The reduction of test pin radius was much greater than the thickness of intermetallic compound layers on the pin surface.
- Three intermetallic compounds, τ_6, τ_5, and τ_2, were observed after 3.5 h of immersion time in the static A390 melt. The thicknesses of intermetallic compounds are constant after 5 h because of the simultaneous dissolution of τ_6 into the melt and the further phase transformation of H13 to τ_2, τ_2 to τ_5, τ_5 to τ_6.
- The melt turbulence accelerated the H13 dissolution dramatically. At higher agitation of the melt, the H13 dissolution was faster, and the intermetallic layers were thinner. Very thin intermetallic compounds, τ_6 (10 μm) and τ_5 (1 μm), were obtained after corrosion test at 175 rpm for 5 h.
- The "washout" or "erosion" in H13 dies, core pins, and shot sleeves is significantly affected by the aggressive diffusion attack of molten aluminum alloys and high velocity of the impinging melt.
- The application of a wear-resistant $Cr_{23}C_6$ coating provided an effective barrier to the molten aluminum attack.

REFERENCES

1. M. Yu and R. Shivpuri, Characterization of Coatings for H13 Dies in Aluminum Die Casting by Accelerated Erosion and Corrosion Tests, *Proceedings of High Temperature Coatings*, (Rosemont, IL), N.B. Dahotre, Ed., TMS, 1994
2. V.G. Rivlin and G.V. Raynor, Critical Evaluation of Constitution of Aluminum-Iron-Silicon System, *Int. Met. Rev.*, No. 3, 1981, p 133
3. M. Yu, Ph.D dissertation, The Ohio State University, Columbus, OH, 1994
4. Y.L. Chu, P. Cheng, and R. Shivpuri, "Erosive Wear in Die Casting," ERC Report ERC/NSM-92-66-C, The Ohio State University, 1992
5. G.M. Goodrich, "Aluminum Die Cast Shot Sleeves—A Metallurgical Study Comparing Long Life and Short Life," Transaction of 16th International Die Casting Congress and Exposition (Detroit, MI), September 30, 1991
6. M.A. Harper and R.A. Rapp, "Codeposition of Chromium and Silicon in Diffusion Coatings for Iron-Base Alloys Using Pack Cementation," Fourth International Conference on Surface Modification Technologies (Paris, France), 1990